Supplementary figures

Endothelial Phospholipase Cγ2 Improves Outcomes of Diabetic Ischemic Limb Rescue Following VEGF Therapy

Yashika Rustagi[1†], Ahmed S Abouhashem[1,2†], Priyanka Verma[1†], Sumit S Verma[1†], Edward Hernandez[1], Sheng Liu[3], Manishekhar Kumar[1], Poornachander R Guda[1], Rajneesh Srivastava[1], Sujit K Mohanty[1], Sedat Kacar[1], Sanskruti Mahajan[1], Kristen E Wanczyk[1], Savita Khanna[1], Michael P Murphy[1], Gayle M Gordillo[1], Sashwati Roy[1], Jun Wan[3], Chandan K Sen[1] and Kanhaiya Singh[1*]

† These authors contributed equally to this work

[1]Indiana Center for Regenerative Medicine and Engineering, Indiana University Health Comprehensive Wound Center, Indiana University School of Medicine, Indianapolis, IN

[2]Sharkia Clinical Research Department, Ministry of Health and Population, Egypt

[3]Center for Computational Biology and Bioinformatics (CCBB), Indiana University School of Medicine, Indianapolis, IN

***Corresponding Author:**

Kanhaiya Singh, PhD
Indiana Center for Regenerative Medicine & Engineering, Department of Surgery, Indiana University School of Medicine, Indianapolis, IN 46202
Tel.: +1 317-278-3411
E-mail: kanh@iu.edu

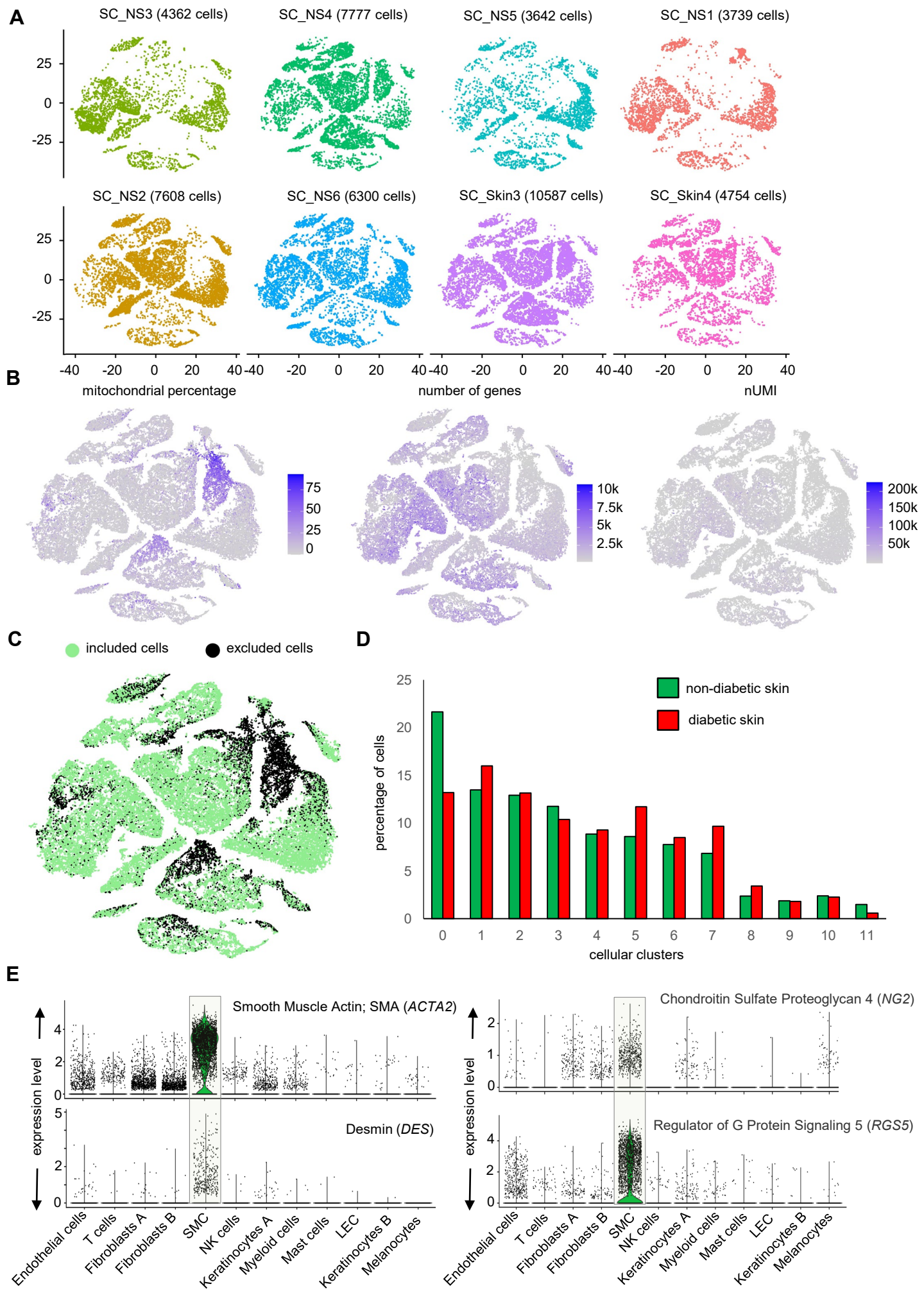
A
SC_NS3 (4362 cells)
SC_NS4 (7777 cells)
SC_NS5 (3642 cells)
SC_NS1 (3739 cells)
SC_NS2 (7608 cells)
SC_NS6 (6300 cells)
SC_Skin3 (10587 cells)
SC_Skin4 (4754 cells)
25
0
-25
-40 -20 0 20 40
mitochondrial percentage
number of genes
nUMI
B
75
50
25
0
10k
7.5k
5k
2.5k
200k
150k
100k
50k
C
included cells
excluded cells
D
non-diabetic skin
diabetic skin
percentage of cells
0 5 10 15 20 25
0 1 2 3 4 5 6 7 8 9 10 11
cellular clusters
E
Smooth Muscle Actin; SMA (ACTA2)
Desmin (DES)
Chondroitin Sulfate Proteoglycan 4 (NG2)
Regulator of G Protein Signaling 5 (RGS5)
expression level
Endothelial cells
T cells
Fibroblasts A
Fibroblasts B
SMC
NK cells
Keratinocytes A
Myeloid cells
Mast cells
LEC
Keratinocytes B
Melanocytes

Supplementary figure 1. Cell filtering and quality control of single cell RNA sequencing data. (**A**) t-distributed stochastic neighbor embedding (t-SNE) projection of raw data with no cells removed. Each cell is represented as a dot. Number of cells detected in each sample before filtering is represented. (**B**) t-SNE plots showing mitochondrial genes percentage (left), total number of detected genes per cell (middle) and number of unique molecular identifiers (nUMI; right). (**C**) t-SNE plot showing the included (green) and excluded cells (black) after performing quality check as described in the methods. (**D**) Bar plot showing the percentage of cells associated with each cell type in both diabetic and non-diabetic skin samples. (**E**) Violin plots representing expression level of pericytes specific genes Smooth Muscle Actin; SMA(*ACTA2*), Desmin (*DES*), Chondroitin Sulfate Proteoglycan 4 (*NG2*) and Regulator of G Protein Signaling 5 (*RGS5*).

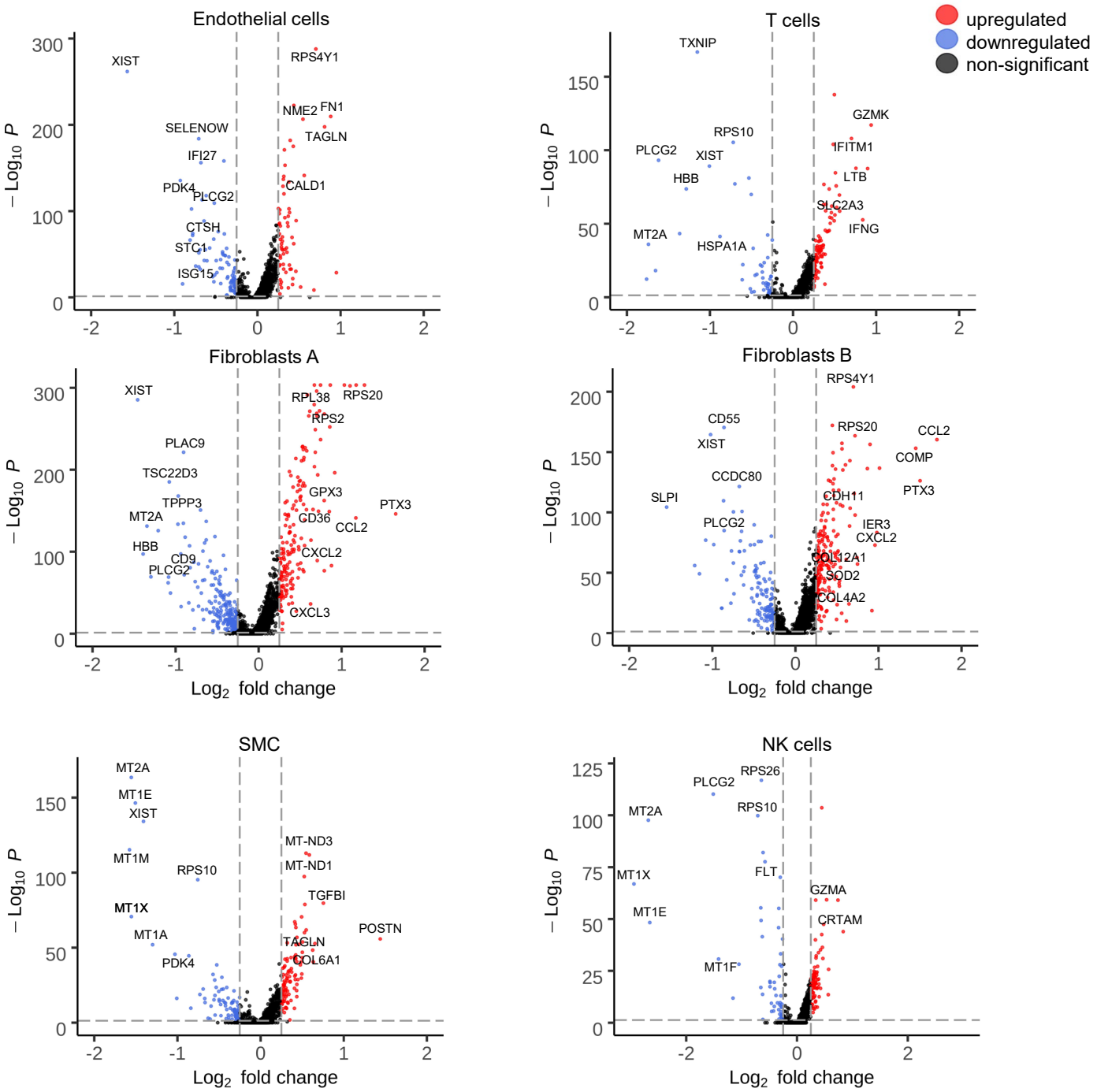

Supplementary figure 2. Differentially expressed genes in different cell types in diabetic skin. Volcano plots showing -log10(FDR) and logFC values for all genes with highlighting for those that are significantly upregulated (red dots; logFC > 0.25) or downregulated (blue dots; logFC < -0.25) with diabetes, as determined by Wilcoxon Rank Sum Test (see details in methods). Genes in black are not significantly changed with diabetes (adjusted p value > 0.05 or logFC is not ±0.25). Each volcano plot corresponds to a different cell type.

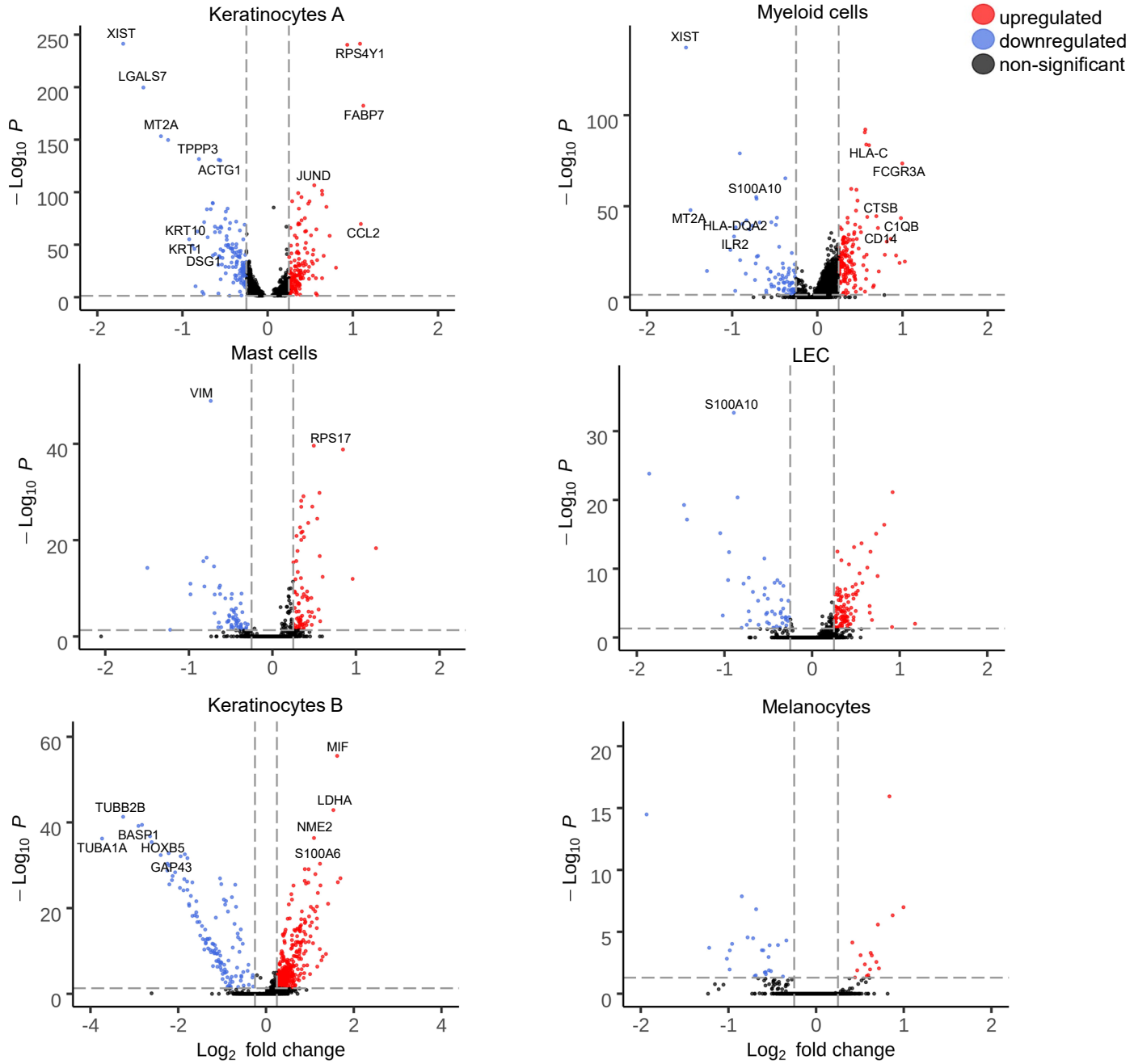

Supplementary figure 3. Continued from Supplementary Figure 2. Differentially expressed genes in different cell types in diabetic skin**.** Volcano plots showing -log10(FDR) and logFC values for all genes with highlighting for those that are significantly upregulated (red dots; logFC > 0.25) or downregulated (blue dots; logFC < -0.25) with diabetes, as determined by Wilcoxon Rank Sum Test (see details in methods). Genes in black are not significantly changed with diabetes (adjusted p value > 0.05 or logFC is not +-0.25). Each volcano plot corresponds to a different cell type.

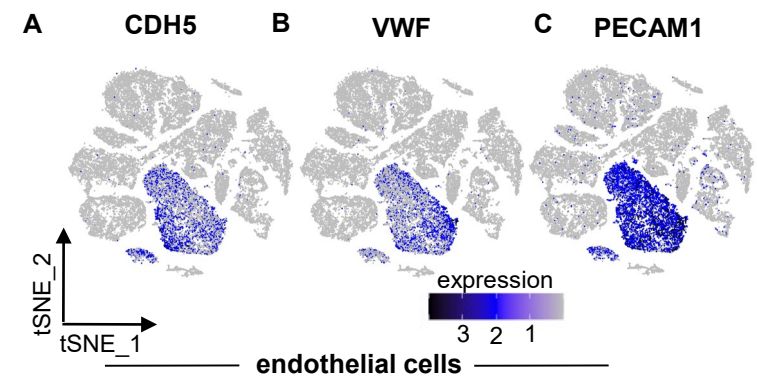

endothelial cells

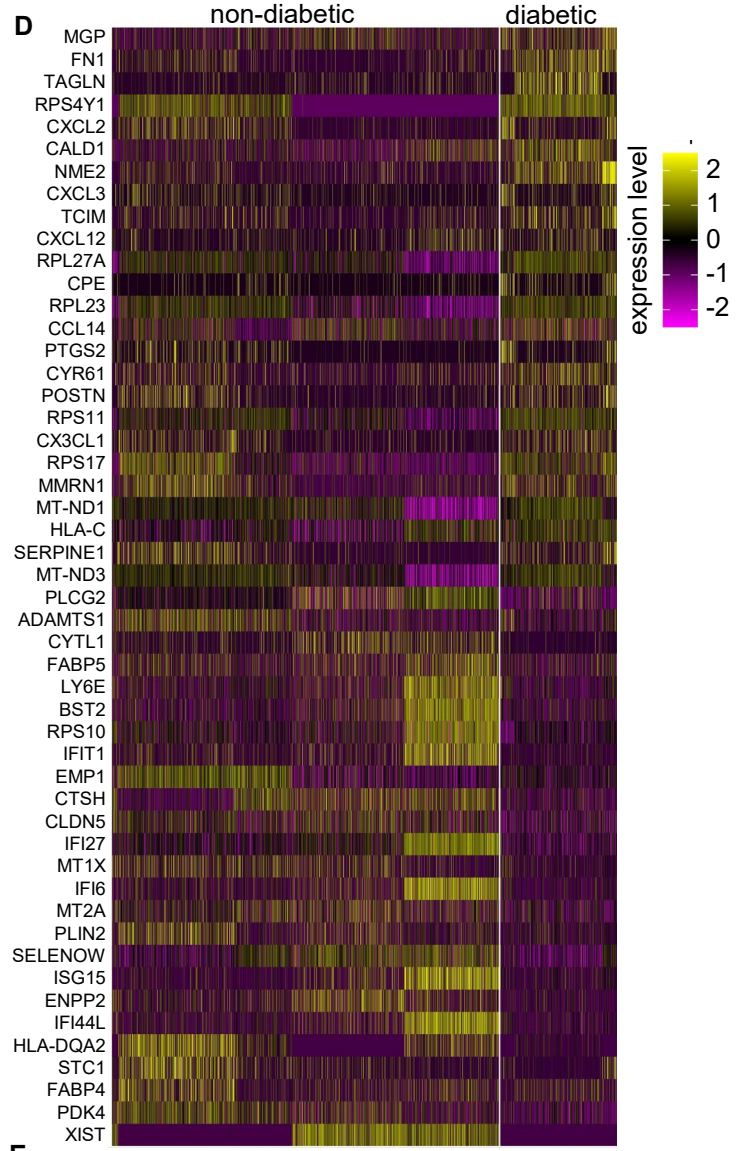

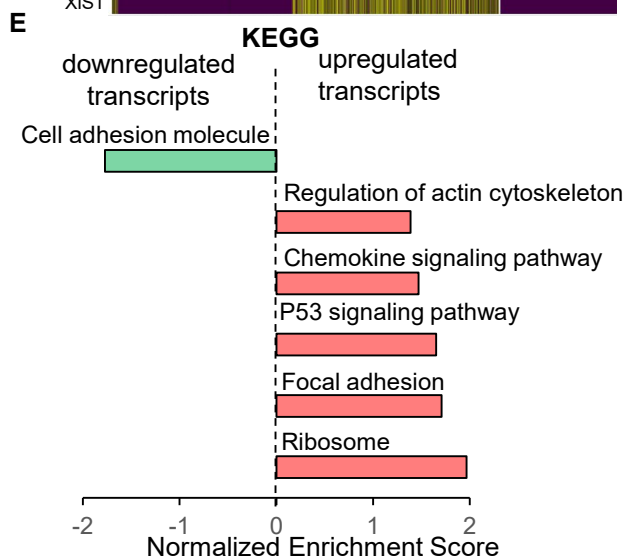

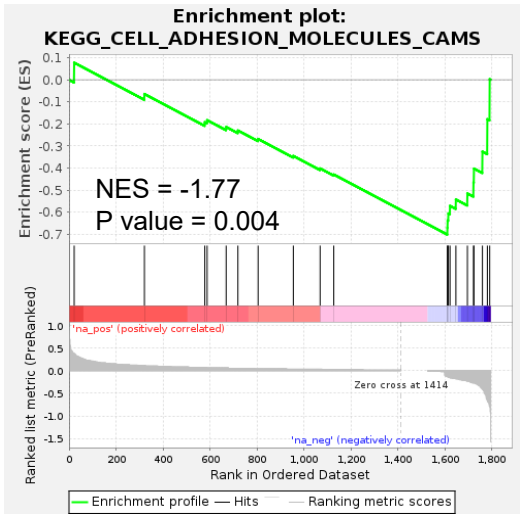

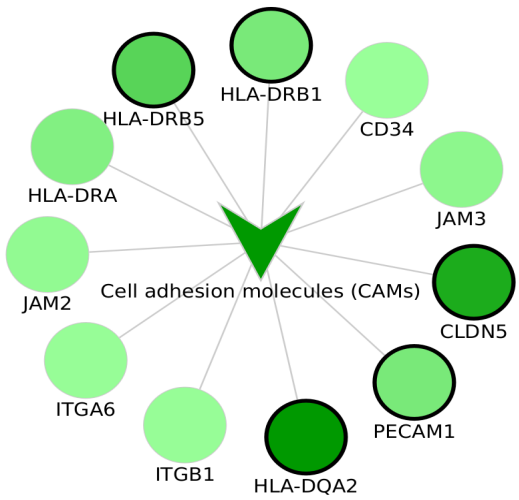

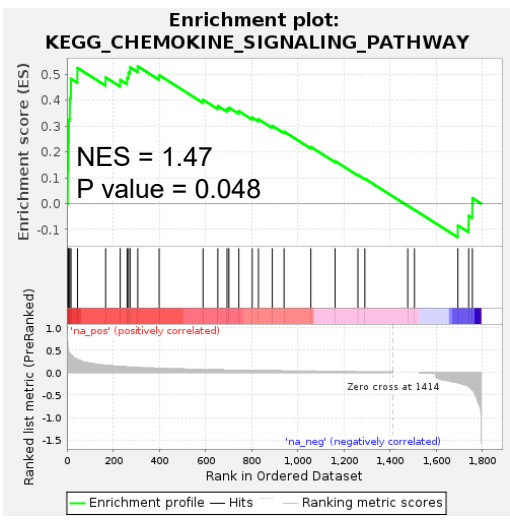

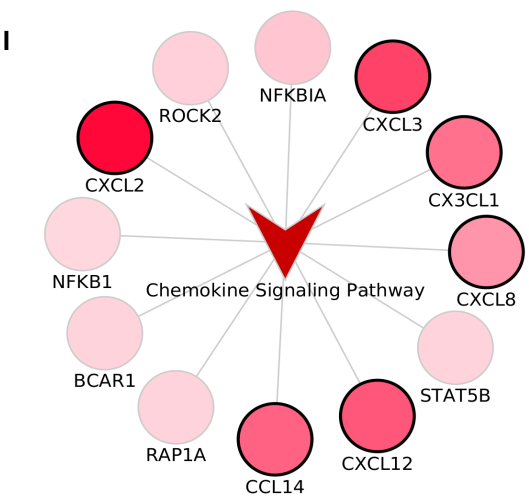

Supplementary Figure 4. Pathways enrichment analysis of endothelial cells differentially expressed genes in diabetic skin. (A) Sub clustering analysis of endothelial cells marked by CDH5 (same image as Fig. 1C), VWF (**B**) and PECAM1 (**C**)**.** (**D**) Heatmap representing top 25 upregulated and downregulated genes in diabetic skin endothelial cell compared to non diabetic skin. **(E)** KEGG pathway analysis showing significant pathways enriched to be downregulated or upregulated in diabetic skin endothelial cells. (F) GSEA analysis showing ribosome pathway to be upregulated and **(G)** Cell adhesion molecule (CAMs) pathway to be downregulated diabetic skin endothelial cells based on normalized enrichment score (NES) (top). Genes identified to contribute in the enrichment score of CAMs with black border surrounding genes which were below the logFC cutoff -0.25 (bottom). Darker greens indicate more downregulation.

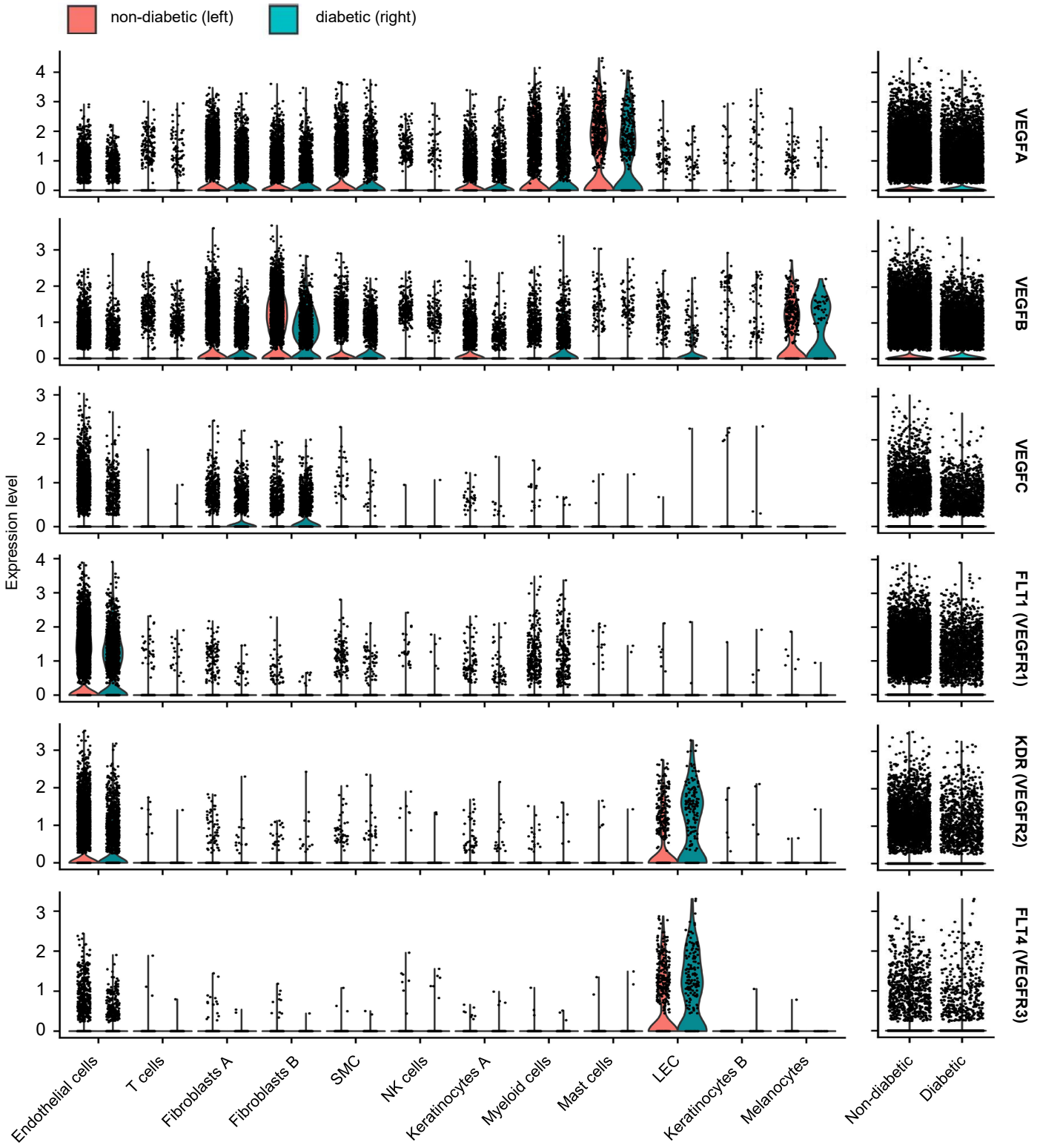

Supplementary figure 5. Expression profiles of VEGF signaling pathway contributing genes in different cell types of diabetic and non-diabetic skin samples. (refer to Figure 3G) (**A**) Violin plots representing expression level of genes contributed in VEGF signaling in each cluster (left) and (**B**) in all cells combined (right) in diabetic and non-diabetic skin.

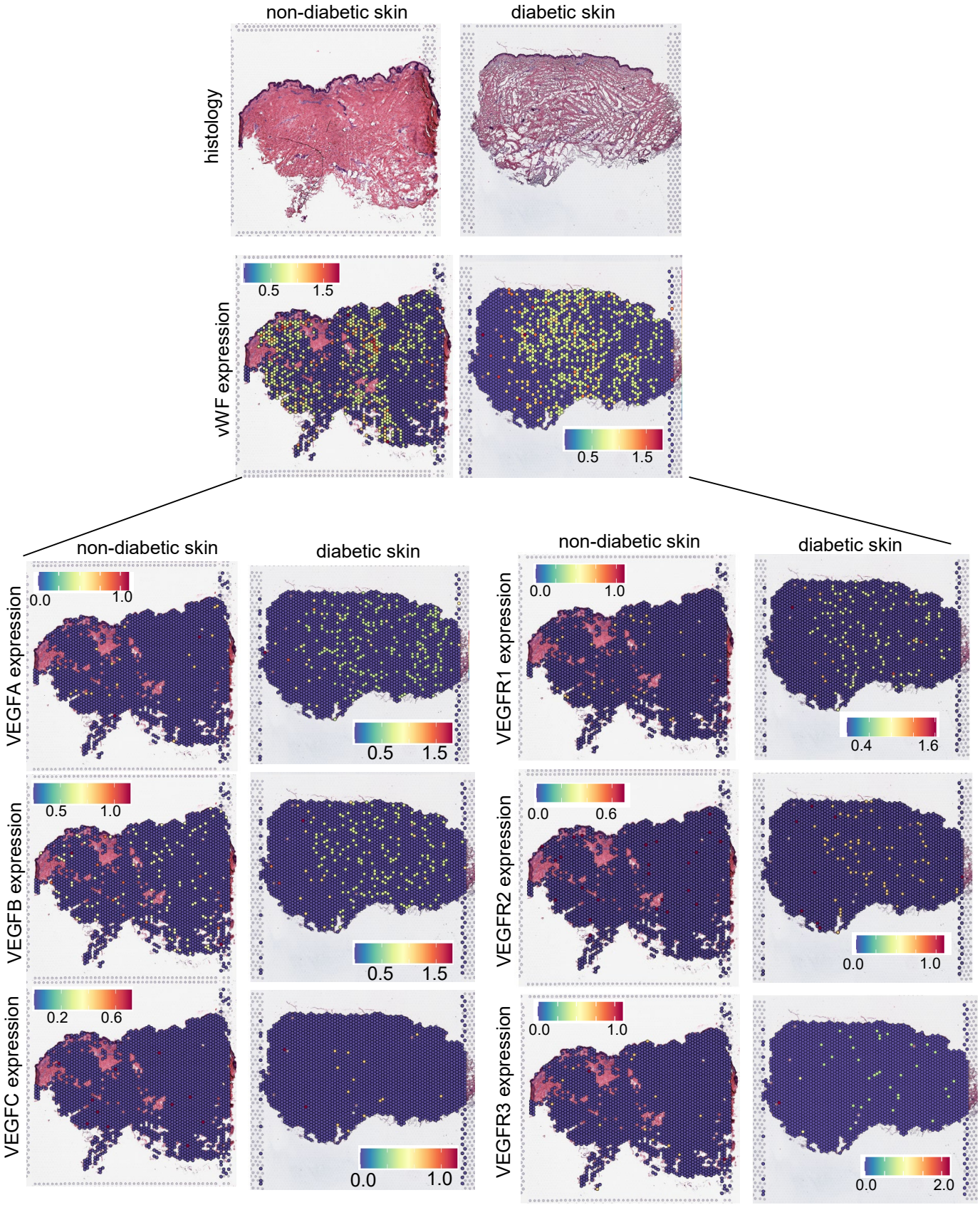

Supplementary figure 6. Spatial transcriptome profile (and localization) of vWF^{+} endothelial cells and VEGF signaling pathway genes (refer. Fig. 4 B-C) of human skin were shown using spatial feature plot function in Seurat. Scale bar for expression levels is provided, where the color towards red indicate high expression.

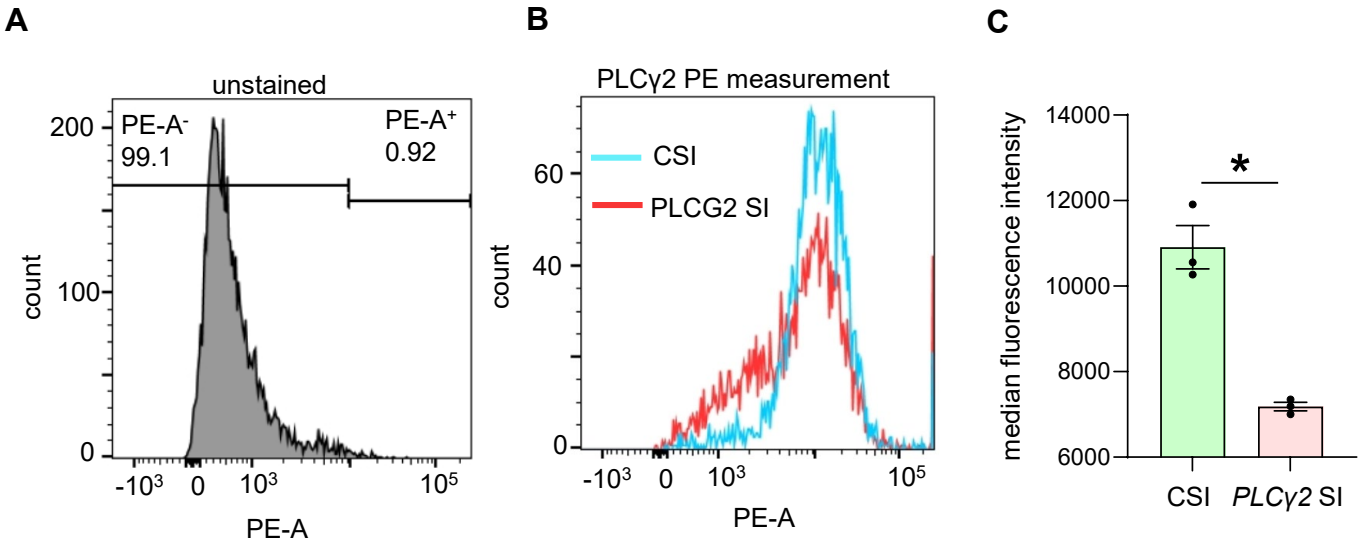

Supplementary figure 7: Flow cytometric validation of *PLCγ2* inhibition using ON-TARGETplus Human PLCG2 siRNA in cultured HMEC cells. **(A)** Histogram showing unstained HMEC cells less no signal in PE channel. (**B**) Figure showing overlapping histograms of *PLCγ2*$^{+}$ HMEC cells treated with either control siRNA (CSI) or *PLCγ2* siRNA. (**C**) Bar plot showing median fluorescence intensity of PLCG2 expression HMEC cells treated with either CSI or *PLCγ2* siRNA. n = 3. *P < 0.05 (Student t test). Data are represented as the mean ± SEM.

A

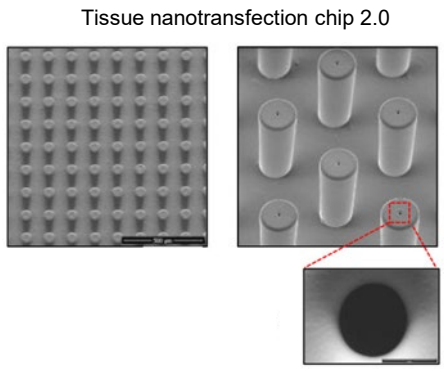

B

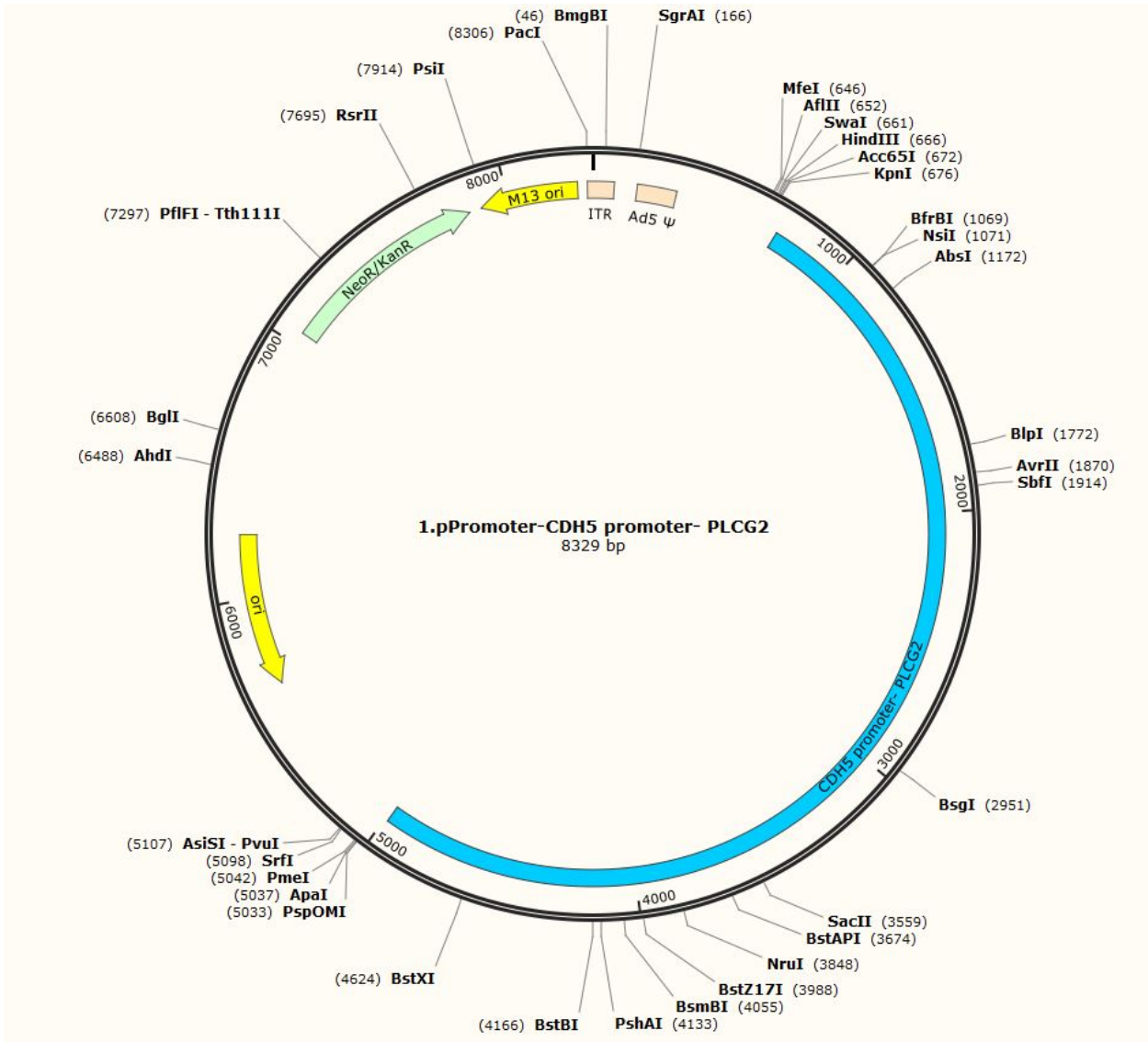

Supplementary Figure 8: TNT2.0 used for delivery of PLCG2 ORF in murine ischemic tissue.(**A**) Representative scanning electron microscopic images of tissue nanotransfection (TNT) chip 2.0. This modified TNT silicon chip ($TNT_{2.0}$) has a longer needle height of 170 μm and a pore diameter of 4 μm. Figure is reprinted (adapted) with permission from Zhou *et al*., ACS Nano 2020, 14, 10, 12732–12748. Copyright (2020) American Chemical Society. (**B**) Plasmid map for endothelial cell (CDH5 promoter driven) targeted overexpression of *PLCγ2* ORF (NM_172285.1) *in vivo*.

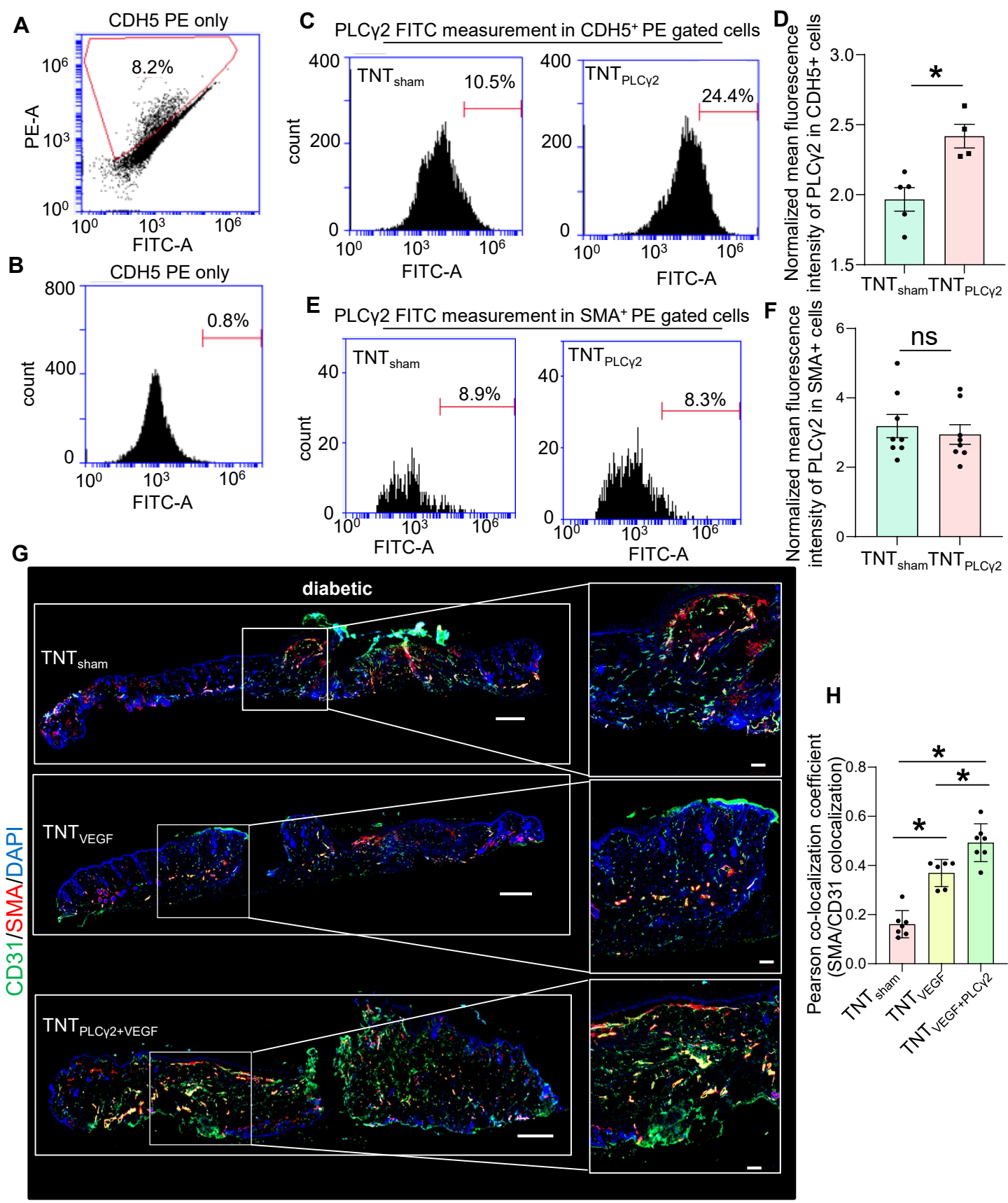

Supplementary figure 9. TNT mediated endothelial PLCG2 overexpression augments VEGF therapy to rescue diabetic ischemic limb. (A) Flow cytometric validation of endothelial specific ($CDH5^+$ promoter driven) overexpression in murine skin through TNT. $CDH5^+$-PE cells were gated (**A**, **B**) and $PLC\gamma2^+$-FITC was measured between sham or endothelial *PLCγ2* ORF transfected murine skin (**C**, **D**). Data represent 4-5 different sites from 3 mice. *P < 0.05 (Student t test). Data are represented as the mean ± SEM. (**E**) Flow cytometry analysis demonstrating overexpression of CDH5+ promoter driven PLCγ2 ORF was not observed in SMA^+-PE cells where the normalized $PLC\gamma2^+$-FITC mean florescence intensity were similar in TNT_{sham} and TNT_{PLCG2} transfected murine skin (**F**). Data represent 8 different sites from 4 mice. P= 0.59 (Student t test). Data are represented as the mean ± SEM. (**G**) Immunohistochemical analysis of $CD31^+/SMA^+$ co-localization in diabetic ischemic limbs of mice treated with sham, VEGF only or VEGF + CDH5 promoter driven (endothelial) PLCγ2 cocktail at day 14 post-surgery and its colocalization coefficient (**H**) n = 6-7. *P < 0.05 (one-way ANOVA, followed by Tukey HSD post hoc test).

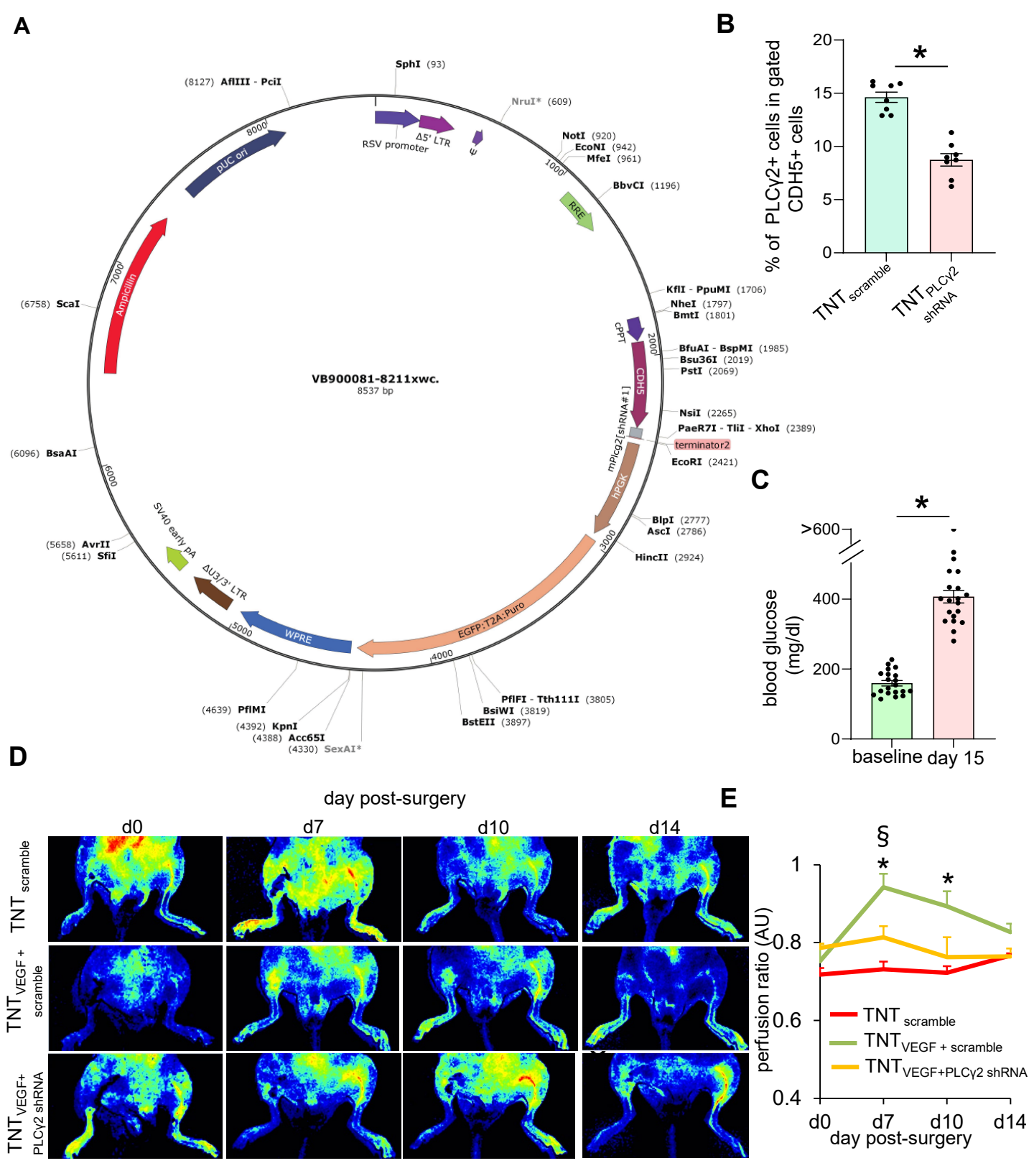

Supplementary figure 10. (A) Plasmid map for endothelial cell (CDH5 promoter driven) targeted PLCγ2 shRNA *in vivo (*target sequence ACCGCAGAGCCCTTCTTATTT, identifier -NM_172285.1-1033s21c1). (**B**) Flow cytometric validation of endothelial specific (CDH5$^+$ promoter driven) downregulation of PLCγ2 in murine skin through TNT. CDH5$^+$-APC cells were gated and PLCγ2$^+$-FITC was measured between scramble or endothelial *PLCγ2* shRNA transfected murine skin. (**C**) Blood glucose level in mice used for shRNA based study before and after injection of streptozotocin (STZ, 50mg/kg). (**D**) PeriMed laser speckle–assisted perfusion images and their analysis (**E**) in ischemic limbs on which TNT procedure was done with scramble, VEGF+scramble or VEGF + CDH5 promoter driven (endothelial) *PLCγ2* shRNA. Perfusion was calculated based on the ratio of the ischemic versus normal/contralateral limb. n = 6-7, *P < 0.05 $TNT_{VEGF+scramble}$ *vs* $TNT_{scramble}$; §P < 0.05 $TNT_{VEGF+scramble}$ *vs* $TNT_{VEGF+PLCγ2\ shRNA}$ (one-way ANOVA, followed by Tukey HSD post hoc test).